GSA DATA REPOSITORY 2020139

Supplementary material for "Ultra-Slow Throw Rates of Polygonal Fault Systems"

James J. King[1], Joe A. Cartwright[1]

[1]*Department of Earth Sciences, University of Oxford, Oxford OX1 3AN, UK*

CHRONOSTRATIGRAPHIC CALIBRATION

The top 250 m of the PFS tier is chronostratigraphically calibrated by eight dated markers from ODP 644 (Fig. DR2). Seven of which were uniquely distinguished and mapable across the study area.

Biostratigraphy - Calcareous Nannofossils

The two youngest stratigraphic markers were biostratigraphically dated by calcareous nannofossil assemblages with the first appearance of E. huxleyi marking the onset of biozone NN21 (0.268 Ma at 22 mbsf), and the last appearance of P. lacunose marking the end of biozone NN19 (0.458 Ma at 51 mbsf) (Eldholm et al., 1987; Berggren et al., 1995; Cohen & Gibbard, 2016). The respective dating of the start of NN21 and end of NN19 have been updated since ODP 644 was published, and we use the current biostratigraphic dating framework outlined by the International Commission on Stratigraphy in our analysis (Cohen & Gibbard, 2016). Diatom, silicoflagellate, radiolarian, planktonic and benthic foraminifer assemblages were also examined but did not yield absolute age dates required for our analysis. Similarly, palynological samples yielded paleoenvironmental insight but no direct age-calibration.

Paleomagnetics

Thirty-four cores from ODP 644 were measured for their natural remanent magnetisation properties on-board the ship using a pass-through cryogenic magnetometer. These results alongside detailed shore-based paleomagnetic analysis of 415 discrete samples using detailed alternating field demagnetisation techniques enabled a complete magnetostratigraphy for the upper Cenozoic that shows exceptional agreement with paleontological analysis (Eldhom et al., 1987; Bleil, 1989). Major geomagnetic boundaries were identified at 83.45 mbsf (Brunhes-Matuyama, C1N-1/C1R-1) and 225.21 mbsf (Matuyama-Gauss, C2R/C2AN-1) (Fig. DR2). Within the Matuyama epoch the top and base Jaramillo were identified at 103.89 mbsf and 111.18 mbsf respectively, and the top and base Olduvai were identified at 166.85 mbsf and 180.81 mbsf respectively (Fig. DR2). The depth in meters below seafloor for these geomagnetic reversals was taken at the midpoint between recorded core samples (Bleil, 1989). The absolute ages of the quaternary paleomagenetic reversals documented in ODP 644 have been updated subsequently to the publishing of Eldholm et al., (1987) and Bleil, (1989) and are summarised in Singer, (2014). We use the updated geomagnetic framework for the respective reversals from Singer (2014) in our analysis.

Seismic-Well Calibration

In the absence of an absolute seismic velocity tie our dated markers have been converted from meters below seafloor to milliseconds (two-way-travel-time, TWT) using a velocity of 1600 m/s as used by Eldholm et al., 1987 (Fig. DR2). The dated horizons have been tied to the seismic at the location of well ODP 644 and mapped to the wiggle apex of the closest seismic reflection. A low velocity estimate of 1500 m/s and a high velocity estimate of 1700 m/s yield a +/- of <10 ms

for the TWT of dated horizons 0.268, 0.458, 0.773, 1.008 Ma and therefore these dated horizons are mapped to an accuracy of +/- one seismic reflection. Dated horizons 1.775, 1.934, and 2.610 Ma have a +/- TWT conversion greater than 10 ms but less than 20 ms given the low and high velocity estimates of 1500 m/s and 1700 m/s respectively and are therefore mapped to an accuracy of +/- two seismic reflections. Assuming a sedimentation rate of around 100 m/Ma (Eldholm et al., 1987) this equates to an error of +/- 0.1 Ma for the seismic calibration of horizons 0.268, 0.458, 0.773, 1.008 Ma and an error of +/- 0.2 Ma for the seismic calibration of horizons 1.775, 1.934, 2.610 Ma respectively. These are represented by vertical error bars in Fig. 3A.

The 1.076 Ma (Base Jaramillo) dated marker cannot be distinguished from the 1.008 (Top Jaramillo) dated marker at the resolution of the seismic data and therefore is not used in our analysis. The 0.773 Ma (Brunhes-Matuyama) dated marker is tied to a laterally discontinuous seismic reflection and is therefore intersected by a small selection of the faults studied. The dated horizons were mapped across the study area using standard 3D tracking techniques in Schlumberger's Petrel software.

Measuring Throw Rates

Time-averaged throw rates were calculated as the change in throw of the 2.61 Ma divided by the elapsed time of 2.61 Myrs. Whereby, the change in throw is measured as the vertical offset in milliseconds of the age-calibrated seismic reflection taken from the apex of the reflection wiggle. In the shallow stratigraphic section calibrated by dated horizons there is limited fault drag, however, where offset reflections are not approximately planar, measurements of throw have been consistently taken to minimise spurious measurement errors by measuring at least one trace

in from the fault plane where the wiggle apex of traces either side are stable. Throw values recorded in milliseconds are converted to meters using a velocity of 1600 m/s as outlined above. Throw measurement are accurate to within +/- 1 m (cf. Townsend et al., 1998). We do not apply a decompaction factor to our throw rates (cf. Taylor et al., 2008) because the ODP 644 porosity versus depth plot (Fig. DR7) exhibits high values (>60%) that do not decrease systematically with depth for the top 250 m of stratigraphy suggestive of little to no compaction over the age-calibrated study interval.

Supplementary Figures

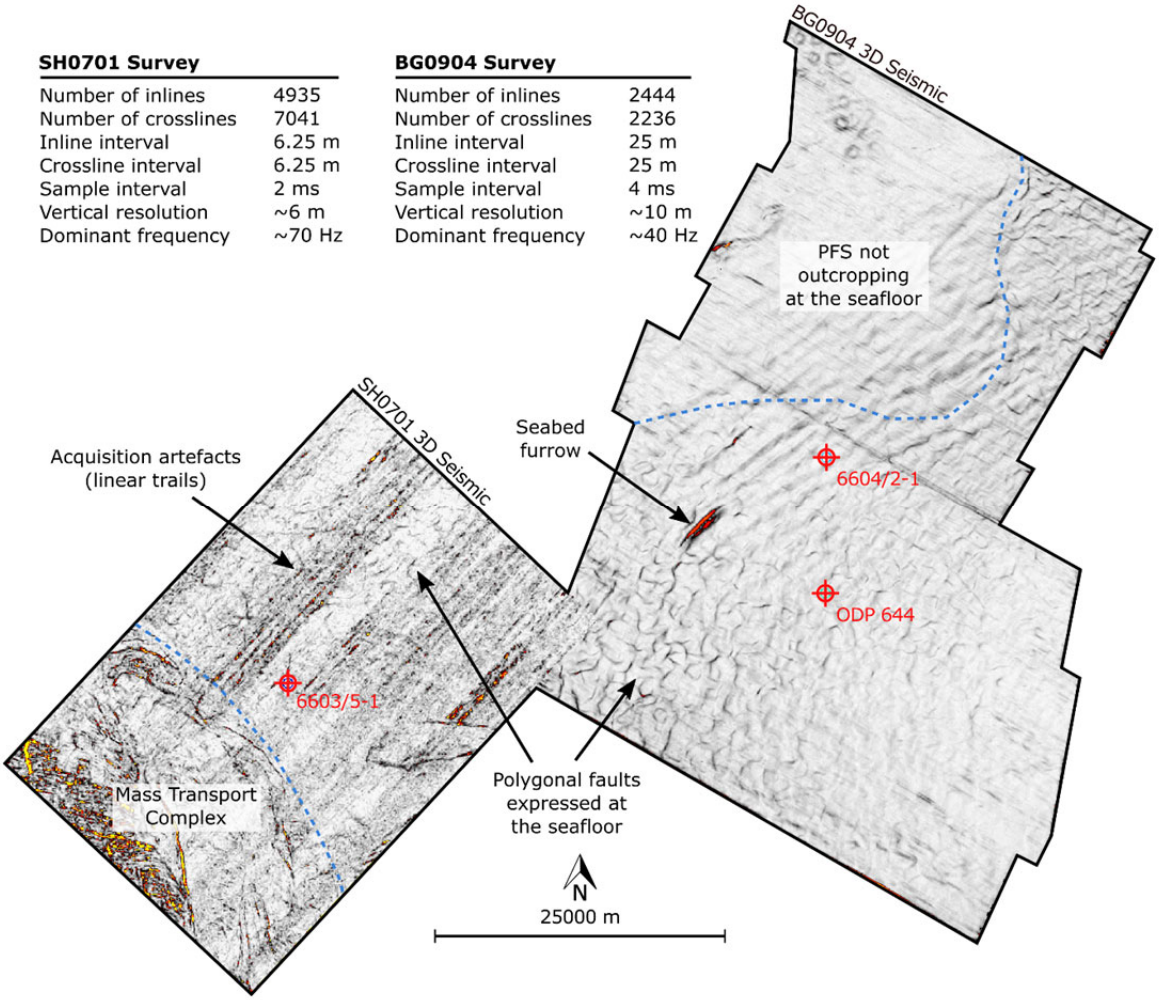

Figure DR1: Seabed maps of the two 3D seismic surveys loacted within the Voring Basin of the Norwegian Sea showing the seabed expression of polygonal faults. ODP and industry wells used to calibrate the litho- and chronostratigraphy are highlighted in red.

ODP 644 - Summary of Dated Horizons				
Depth (mbsf)	**Depth TWT (ms) v = 1600 m/s**	**Age (Ma)**	**Dating Technique**	**Description**
0	1662.8	0.000	-	Seabed
22.00	1690.3	0.268	Calcareous nannofossils	FAD *E. huxleyi* (NN21)
51.00	1726.6	0.458	Calcareous nannofossils	LAD *P. lacunosa* (NN19/20)
83.45	1767.1	0.773	Paleomagnetics	Brunhes-Matuyama - C1N-1/C1R-1
103.89	1792.7	1.008	Paleomagnetics	Top Jaramillo - C1R-1/C1N-2
111.18	1801.8	1.076	Paleomagnetics	Base Jaramillo - C1N-2/C1R-2
166.85	1871.4	1.775	Paleomagnetics	Top Olduvai - C1R-2/C2N
180.81	1888.8	1.934	Paleomagnetics	Base Olduvai - C2N/C2R
225.21	1944.3	2.610	Paleomagnetics	Matuyama-Gauss - C2R/C2AN-1

Figure DR2: Summary table of dated horizons from ODP 644. See chronostratigraphic calibration section above for detailed description.

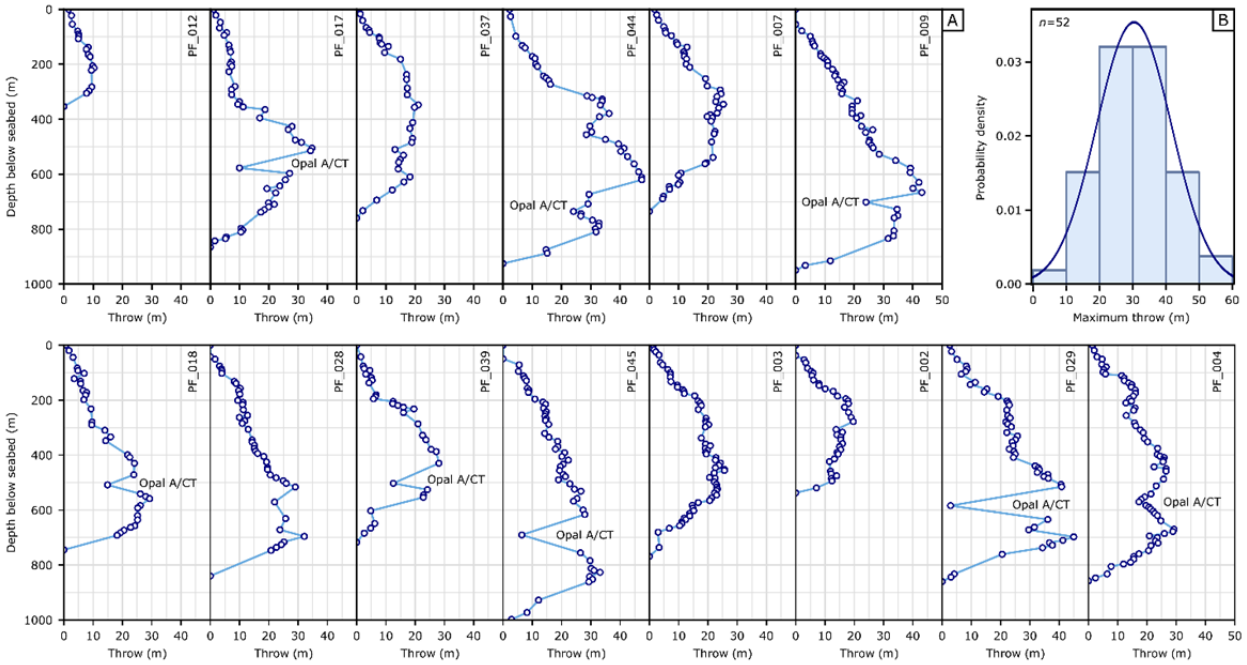

Figure DR3: (A) Throw versus depth plots for the same 14 faults exhibited in Figure 3 (main text). (B) Probability density function of maximum throw for 52 faults.

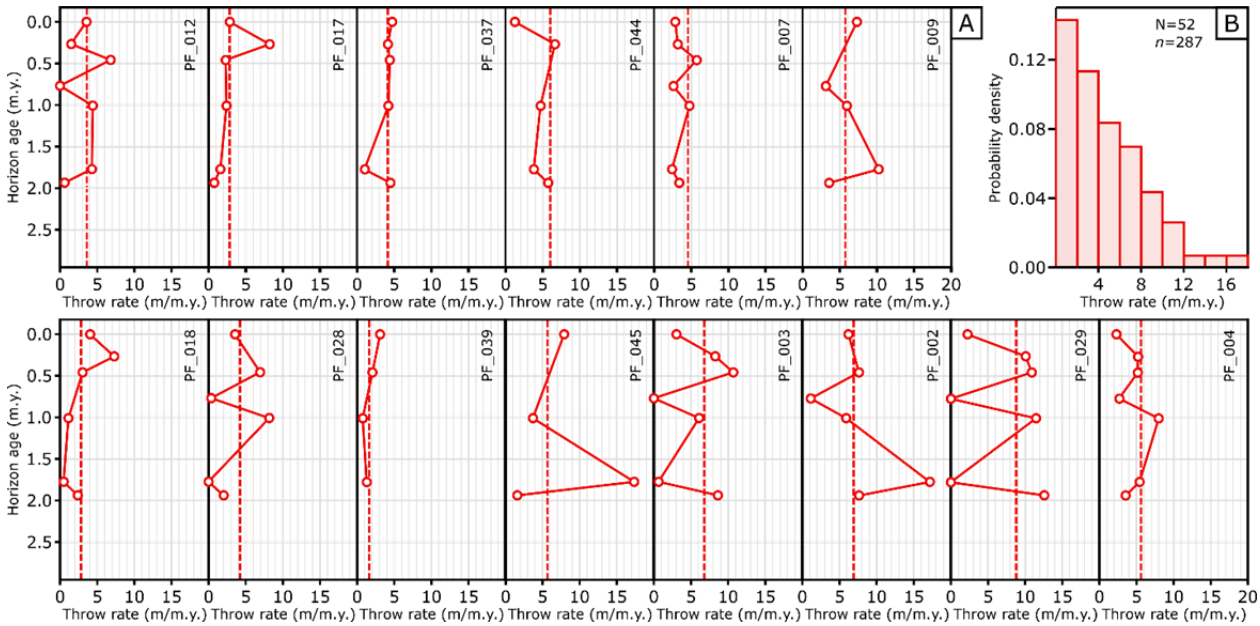

Figure DR4: (A) Throw rate versus horizon age plots for the same 14 faults exhibited in Figure 3 (main text). Throw rate is calculated as the change in throw divided by the change in time (horizon age) between adjacent data points of known age. The dashed lines represent the time-averaged throw rate for each fault taken as the throw at the 2.61 Ma horizon divided by time. (B) Probability density function of short-term throw rates (n=287) for 52 faults (N=52).

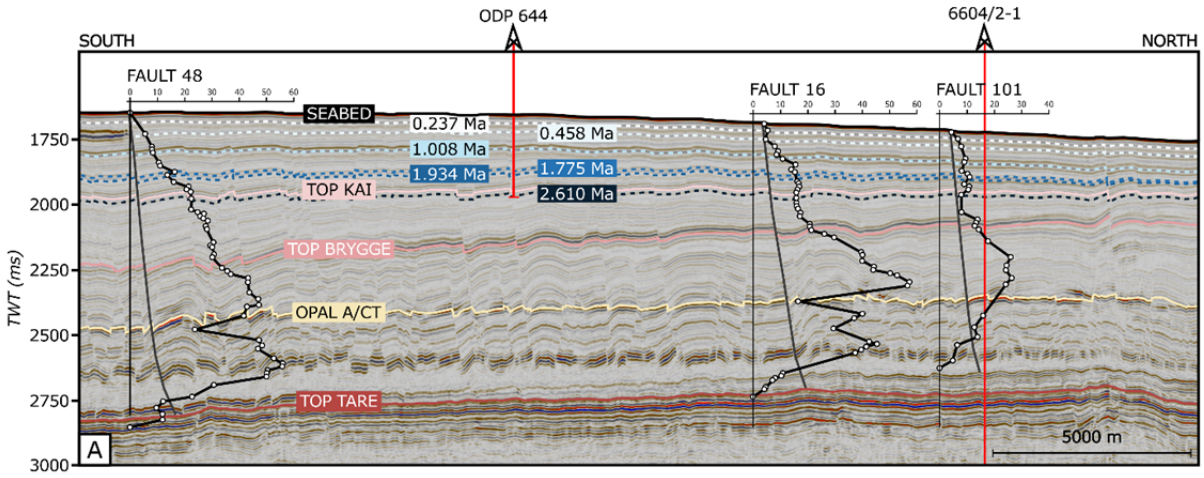

Figure DR5: Extended seismic profile from Fig. 1B with three throw versus depth plots superimposed.

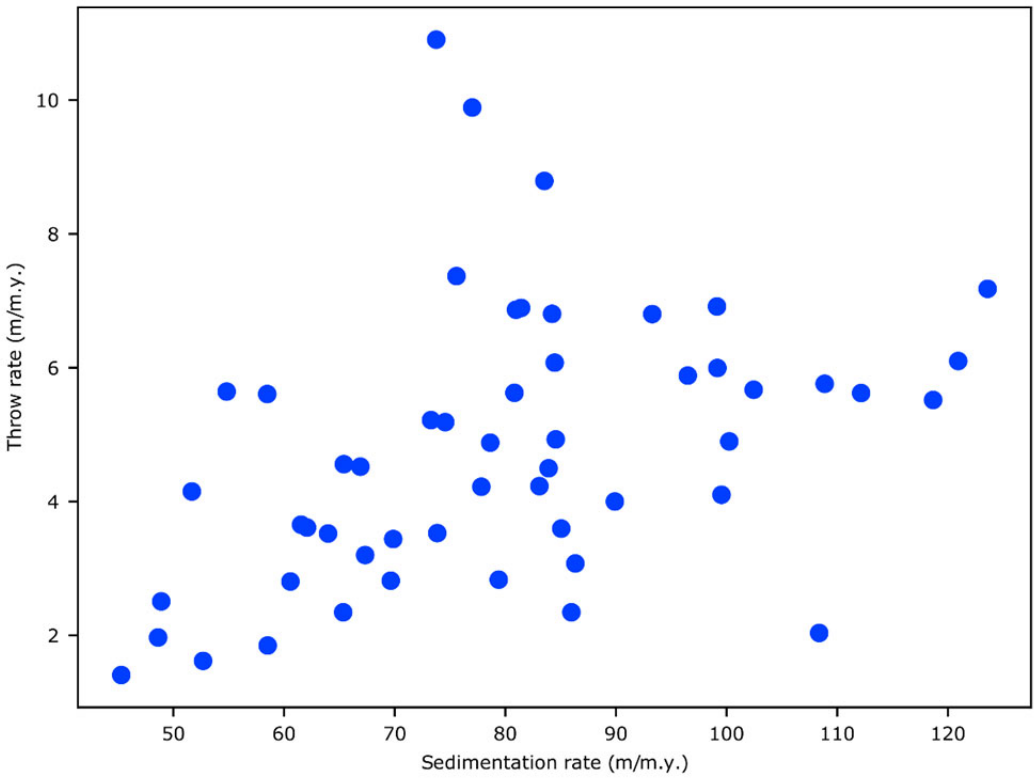

Figure DR6: Time averaged sedimentation rates outpace throw rates by at least one order of magnitude.

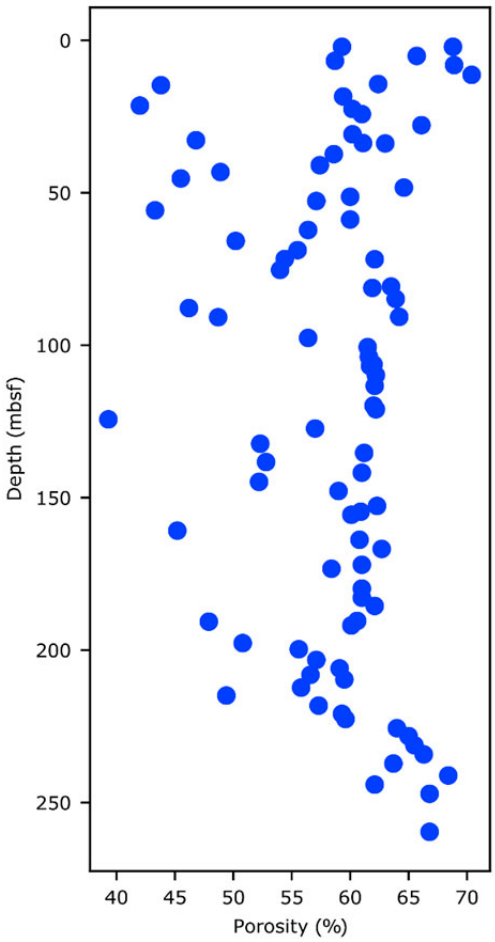

Figure DR7: ODP 644 - porosity versus depth profile from Eldholm et al., (1987).

REFERENCES

Berggren, W.S., Hilgen, F.J., Langereis, C.G., Kent, D.V., Obradovich, J.D., Raffi, I., Raymo, M.E. and Shackleton, N.J. (1995). Late Neogene chronology: new perspectives in high-resolution stratigraphy. Geological Society of America Bulletin 107, 1272-1287

Bleil, U. (1989). Magnetostratigraphy of Neogene and Quaternary sediment series from the Norwegian Sea: Ocean Drilling Program, Leg 104. *In* Eldholm, O., Thiede, J., Taylor, E., et al., *Proc. ODP, Sci. Results,* 104: College Station, TX (Ocean Drilling Program), 829–901. doi:10.2973/odp.proc.sr.104.181.1989

Cohen, K. M., & Gibbard, P. L. (2016). Global chronostratigraphical correlation table for the last 2.7 million years v. 2016a. Cambridge: Subcommission on quaternary Stratigraphy, International Commission on Stratigraphy; 2016.

Eldholm, O., Thiede, J., Taylor, E. (1987). Site 644: Norwegian Sea. In *Proceedings of the Ocean Drilling Program, 104 Initial Reports*. Ocean Drilling Program. https://doi.org/10.2973/odp.proc.ir.104.105.1987

Singer, B. S. (2014). A Quaternary geomagnetic instability time scale. *Quaternary Geochronology*, *21*, 29-52. https://doi.org/10.1016/j.quageo.2013.10.003

Taylor, S. K., Nicol, A., & Walsh, J. J. (2008). Displacement loss on growth faults due to sediment compaction. Journal of Structural Geology, 30(3), 394-405. doi.org/10.1016/j.jsg.2007.11.006

Townsend, C., Firth, I. R., Westerman, R., Kirkevollen, L., Hårde, M., & Andersen, T. (1998). Small seismic-scale fault identification and mapping. *Geological Society, London, Special Publications*, *147*(1), 1–25. https://doi.org/10.1144/gsl.sp.1998.147.01.02.